J Membrane Biol (2008) 222:115–125
DOI 10.1007/s00232-008-9104-x

Tubulin as a Binding Partner of the Heag2 Voltage-Gated Potassium Channel

Kate Bracey · Min Ju · Chenguang Tian · Louisa Stevens · Dennis Wray

Received: 18 September 2007 / Accepted: 14 March 2008 / Published online: 6 May 2008

Abstract The aim of this work was to investigate interactions of the human ether-a-go-go channel heag2 with human brain proteins. For this, we used heag2–GST fusion proteins in pull-down assays with brain proteins and mass spectrometry, as well as coimmunoprecipitation. We identified tubulin and heat shock 70 proteins as binding to intracellular C-terminal regions of the channel. To study functional effects, heag2 channels were expressed in *Xenopus laevis* oocytes for two-electrode voltage clamping. Coexpression of α-tubulin or the application of colchicine significantly prolonged channel activation times. Application at different times of colchicine gave similar results. The data suggest that colchicine application and tubulin expression do not affect heag2 trafficking and that tubulin may associate with the channel to cause functional effects. Coexpression of heat shock 70 proteins had no functional effect on the channel. The role of tubulin in the cell cytoskeleton suggests a link for the heag2 channel in tubulin-dependent physiological functions, such as cellular proliferation.

Keywords Heag2 channel · Tubulin · Potassium channel

Introduction

Voltage-gated potassium channels are of fundamental importance in the functioning of excitable cells due to their selectivity for the movement of potassium ions across the membranes of these cells. The physiological functions of these channels are wide-ranging, including control of the electrical activity of cells, control of hormone release and involvement in cell proliferation. The critical importance of these channel proteins is demonstrated by the number and diversity of inherited disorders associated with their dysfunction (Bracey and Wray 2006).

The ether-a-go-go (eag) potassium channel family shares the membrane-spanning architecture and channel structure predominantly seen in voltage-gated potassium channels. Four α-subunits, each comprising six transmembrane domains (S1–S6), the pore (P) region and the intracellular termini, form the channel protein. The S1–S4 transmembrane domains are the voltage sensor, the P region forms the potassium ion selectivity filter and the rest of the pore is lined by S6 (Yellen 2002). A distinguishing characteristic of the eag channel family is the long intracellular N and C termini; a Per-Arnt-Sim (PAS) domain is present in the N terminus and a cyclic nucleotide binding domain (cNBD) in the C terminus (Bauer and Schwartz 2001).

The mammalian eag channel family includes eight members, and the present study focuses on the human eag2 channel (heag2) (Ju and Wray 2002; Schönherr et al. 2002). The heag2 channels are extensively expressed in the brain (as well as other tissues such as heart and skeletal muscle) (Ju and Wray 2002) and display outwardly rectifying, noninactivating potassium currents. Extensive electrophysiological characterization has been carried out on these channels, identifying the functional importance of particular domains of the channel in determining these electrophysiological characteristics (Ju and Wray 2006). In the case of the heag1 channel, the cytoskeletal proteins of microfilaments and microtubules have been identified as influencing the electrophysiological properties (Camacho et al. 2000; Toral et al. 2007). This information, combined with research showing that the heag1 channel introduces oncogenic properties to cells (Pardo et al.

K. Bracey · M. Ju · C. Tian · L. Stevens · D. Wray (✉)
Faculty of Biological Sciences, University of Leeds,
Leeds LS2 9JT, UK
e-mail: d.wray@leeds.ac.uk

1999; Farias et al. 2004; Mello de Queiroz et al. 2006), indicates a physiological function for the heag1 channel in cellular proliferation.

The aim of the current work was to investigate interactions of the heag2 channel with human brain proteins and subsequently to investigate any functional effects of these interacting proteins on the channel. These aims were achieved by pull-down assays using GST fusion proteins with fragments of the heag2 channel, followed by identification of binding partners by mass spectrometry. Functional effects of identified binding partners were characterized by coexpression in oocytes followed by electrophysiology.

Methods

Molecular Biology

The heag2 cDNA (accession number AF472412) in pGem-He-Juel was already available from our previous work (Ju and Wray 2002). The heag2 cDNA was subcloned into the pcDNA3 vector between the *Kpn*I and *Not*I restriction sites. GST fusion constructs were made with fragments of the heag2 channel using overhang polymerase chain reaction (PCR), as previously described (Ju et al. 2003). *Eco*RI and *Xho*I restriction sites were used to subclone the PCR products into the pGEX-4T-3 vector (Amersham Biosciences, Little Chalfont, UK). The GST fusion constructs were made using the following C-terminal regions of heag2: the S6-cNBD linker (residues 471–549), the cNBD (residues 550–650), the variable domain (VD) (residues 717–826) and the end of the C terminus (residues 909–978). These fragments were chosen according to structurally distinct large domains likely to retain the native conformation. For instance, the cNBD domain (and linker to S6) is homologous to that found in the HCN channel, for which the conformation has been determined by X-ray crystallography (Zagotta et al. 2003). For expression in oocytes, the human α-tubulin cDNA pEGFP-Tub (Clontech, Saint-Germain-en-Laye, France) was subcloned into the oocyte expression vector pGem-He-Juel, using overhang PCR with *Bam*HI and *Xba*I restriction sites. The heat shock cognate 71-kDa protein Hsc71 cDNA (gift from R. Morimoto, Northwestern University, IL, USA) was also subcloned into pGem-He-Juel using overhang PCR with *Bam*HI and *Xba*I restriction sites. Myelin basic protein cDNA was subcloned into pGem-He-Juel using the *Eco*RI restriction enzyme. All constructs were confirmed by dideoxy sequencing (Lark Technologies, Takeley, UK). For expression in oocytes, all of the cDNAs in pGem-He-Juel were linearized using *Not*I restriction enzyme, and capped cRNA was transcribed in vitro using the T7 promoter (Megascript; Ambion, Warrington, UK).

Protein Expression

The C-terminal heag2-GST constructs were transformed in BL21 *Escherichia coli* cells (Promega, Southampton, UK), and large-scale cultures were grown for 5 h. Protein expression was induced by addition of 0.25 mM isopropylthiogalactoside (IPTG) followed by a 90-min incubation at 37°C. Cells were lysed by repetitive freeze/thaw, and the soluble protein fraction was separated from the insoluble material by centrifugation.

Protein Purification

Heag2–GST fusion proteins were purified from the soluble fraction as follows. Glutathione sepharose bead slurry (50%, 20 µl; Amersham Biosciences) was added to 1 ml of lysate. After incubating at room temperature for 5 min, the mixtures were centrifuged for 5 s at 13,000 rpm to pellet the beads, which were then washed three times in 1x phosphate-buffered saline (PBS). PBS (10 µl) was added, and the mixtures were incubated for 5 min at room temperature. The samples were again washed and centrifuged three times before the GST fusion proteins were eluted from the beads by adding 10 µl elution buffer (Amersham Biosciences). The purified samples were subjected to 12% sodium dodecyl sulfate-polyacrylamide gel electrophoresis (SDS-PAGE) and verified using Western blotting with a mouse anti-GST primary antibody (0.1 µg/ml; Novagen, Nottingham, UK) and goat anti-mouse secondary antibody (1 µg/ml, Novagen), with detection using horseradish peroxidase (HRP) and ECL on film, enhanced with SuperSignal HRP substrate (Novagen).

Binding Assay

Heag2–GST fusion proteins (soluble fraction 1 ml) were mixed with glutathione sepharose slurry, centrifuged and washed as above. Then, 10 µl of the human brain protein medley (BD Biosciences, Oxford, UK; 10 mg/ml) was added, and the mixtures were incubated for 5 min at room temperature. After washing and centrifuging three times, proteins were eluted from the glutathione sepharose beads as before and run on 12% SDS-PAGE gels. Coomassie-stained protein bands were excised from the SDS-PAGE gels and subjected to trypsin digest. The resulting peptide mixture of each excised band was analyzed by matrix-assisted laser desorption ionization/time of flight (MALDI-TOF) mass spectrometry (Venter et al. 2002). The proteins corresponding to the peptide mass spectra were identified using the Mascot database (Perkins et al. 1999).

Immunoprecipitation

HEK293 cells were transfected using lipofectamine (Invitrogen, Paisley, UK) with heag2 cDNA or cotransfected with heag2 and Hsp70 cDNAs (the latter clone, in pcDNA3, was a gift from D. Devys, C. U. Strasbourg, France). Cells were then lysed in 200 µl cell lysis buffer (50 mm Tris-HCl, 150 mm NaCl, 5 mm EDTA and 1% Triton X-100 with protease inhibitors). After centrifugation at 13,000 rpm for 10 min at 4°C, 10 µl of anti α-tubulin antibody (1.25 µg/ml; Sigma, Poole, UK) or anti-Hsp70 antibody (1–10 µg/ml; Abcam, Cambridge, UK) was added to the supernatant and incubated at 4°C overnight. Protein A agarose beads (100 µl) were then added to the protein samples and, after incubating at 4°C, centrifuged and washed three times in 1 ml of cell lysis buffer. Proteins were eluted from the beads by addition of 60 µl sample buffer and boiling for 5 min. The protein samples were then subjected to SDS-PAGE and transferred to nitrocellulose membranes for Western blotting with an anti-heag2 antibody (4 µg/ml; Alomone Labs, Jerusalem, Israel).

Electrophysiology

Xenopus laevis oocytes were prepared and injected with RNA for heag2 (7 ng), heag2/α-tubulin (7 + 7 ng), heag2/MBP (7 + 7 ng) or heag2/Hsc71 (7 + 7 ng) in 50 nl. Oocytes were then incubated for 2 days in a modified Barth's solution containing (in mM) 88 NaCl, 1 KCl, 2.4 $NaHCO_3$, 0.82 $MgSO_4$, 0.4 $Ca(NO_3)_2$, 7.5 Tris HCl (pH7.6), penicillin (100 U/l) and streptomycin (1 mg/l). For the chronic colchicine exposure experiments, oocytes were incubated in the modified Barth's solution which also contained colchicine (50 µM) for different time periods during the 2-day incubation of oocytes (for 1–5, 1–24, 24–48 and 43–48 h). For experiments with paclitaxel, oocytes were incubated in modified Barth's solution containing paclitaxel (500 nM) for the first 24 h of the 2-day incubation period after heag2 RNA injection. Currents were recorded using two-electrode voltage clamping as previously described (Ju and Wray 2006). Oocytes were held in a 50-µl chamber and continuously perfused with a solution containing (in mM) 2 KCl, 115 NaCl, 10 HEPES and 1.8 $CaCl_2$, at pH 7.2, 22–24°C. Currents were recorded with a GeneClamp 500 amplifier (Axon, Egham, UK), and signals were sampled at 4 kHz and filtered at 2 kHz. To obtain current–voltage (*I–V*) relationships, 500-ms depolarizing pulses at a frequency of 0.1 Hz were applied from a holding potential of −80 m*V* in 10-m*V* increments from −70 to 70 m*V*. All currents were leak-subtracted using 20 10-m*V* hyperpolarizing steps. For experiments to study the acute action of colchicine, 500-ms depolarizing pulses were applied at a frequency of 0.1 Hz from a holding potential of −80 to 40 m*V* during the application of colchicine (50 µM) in the bath. Activation times, $t_{10-90\%}$, were taken as the time for currents to rise from 10% to 90% of maximum current. To minimize effects due to variations in heag2 expression, for each batch of oocytes, cells expressing heag2 alone were always recorded from alongside cells coexpressing tubulin, heat shock protein or myelin basic protein. Student's *t*-test was used to test for statistical significance.

Results

Binding Studies

In order to identify proteins binding to the heag2 channel, GST fusion proteins incorporating parts of the C terminus were expressed, purified and then mixed with a human brain protein medley. Proteins binding to the C-terminal regions were then isolated by running SDS-PAGE gels and protein band excision. After tryptic digest, the proteins were identified using MALDI-TOF mass spectrometry. Binding was confirmed using coimmunoprecipitation.

Protein Purification

Four regions of the C terminus of heag2 (S6-cNBD, cNBD, VD, End-C; see "Methods") were expressed as heag2–GST fusion proteins in *E. coli*. These GST fusion proteins were purified using glutathione to bind to the GST fusion proteins; unbound proteins were extensively washed from the samples. Purified samples (approx. 1 µg) were run on 12% SDS-PAGE gels (Fig. 1). Each of the four heag2–GST fusion proteins gave a clear band after purification at the expected size for each GST fusion construct (example shown for GST-VD, Fig. 1C), and a clear band for expression of GST protein alone (run alongside as a positive control, Fig. 1B). The negative control (the soluble fraction from uninduced cells, Fig. 1A) showed no binding of cellular proteins to the glutathione beads.

The identity of the protein bands was established by Western blotting using anti-GST antibody (Fig. 1D). The bands shown in the Western blot correspond to the SDS-PAGE analysis of the GST fusion proteins, including the GST band in lane 2. Two bands were observed for S6–cNBD–GST (also observed on SDS-PAGE gels), corresponding to the fusion protein and cleaved GST product (most likely due to protease cleavage at the thrombin site).

Binding Study

The binding study was carried out with the human brain protein medley to identify binding partners from this medley for each of the four C-terminal heag2–GST fusion

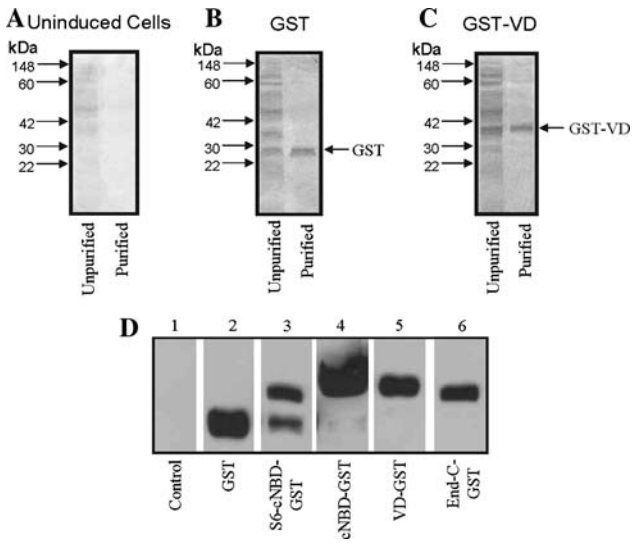

Fig. 1 Purification of C-terminal heag2–GST fusion proteins. The GST fusion proteins were purified from the soluble fraction after *E. coli* cell lysis using glutathione sepharose beads and resolved by SDS-PAGE visualized with Coomassie blue. Examples are shown for (**A**) negative control of soluble protein fraction from uninduced BL21 cells, (**B**) GST alone (29 kDa) and (**C**) GST–VD fusion protein (38 kDa). (**D**) A Western blot using anti-GST antibody is shown, with lanes corresponding to the purified fractions indicated in the figure

proteins. An example SDS-PAGE gel is shown in Fig. 2B for the End–C–GST fusion construct (protein concentration approx. 1 μg). Upon mixing this fusion protein with the brain medley, proteins binding to the heag2–GST fusion protein were evident as extra bands compared with the unmixed GST fusion protein (Fig. 2B). Further extra bands (not seen in the figure) were visualized when the SDS-PAGE gel was examined using a light source. As can be seen in Fig. 2A, no extra bands were seen in the gel for GST alone, indicating lack of binding to the GST tag itself. Also, there were no extra bands in gels for uninduced cells (data not shown).

In order to identify the extra bands found upon mixing with the brain protein medley, digestion with trypsin followed by MALDI-TOF mass spectrometry was used. An example mass spectrograph is shown in Fig. 2C, with identified proteins shown in Fig. 2D (in this case the band comprised a mixture of α- and β-tubulin at almost the same molecular weight). Each of the heag2–GST fusion protein samples was found to bind to a number of proteins from the human brain protein medley. Some of the extra bands were identified as human proteins, and others were due to *E. coli* proteins. For all of the GST fusion constructs, a summary of the identified human proteins is shown in Table 1. For S6–cNBD, the identified proteins corresponded to α- and β-tubulins and Hsc71 protein. For the cNBD fusion construct, fragment masses indicated binding of α- and β-tubulins and myelin basic protein; for the VD construct, α- and

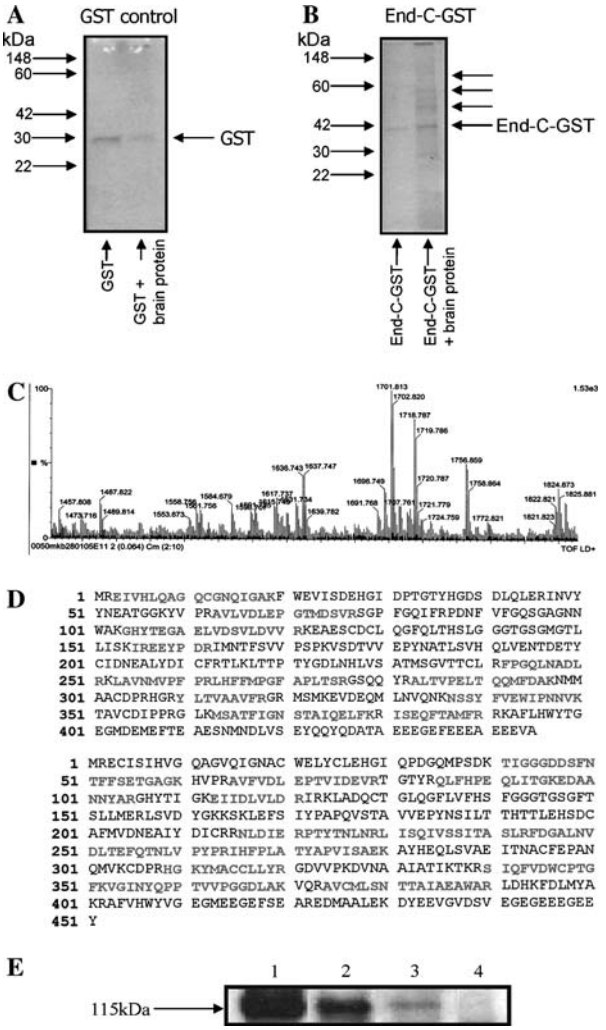

Fig. 2 Identification of binding partners. (**A**) SDS-PAGE gel (stained with Bio-Safe Coomassie; Bio-Rad, Hemel Hempstead, UK) of GST protein to identify any false binding partners. *Lane 1*, purified GST protein; *lane 2*, GST protein mixed with brain protein medley, showing only a clear band corresponding to the expected 29-kDa size. (**B**) Example of SDS-PAGE gel (stained with Bio-Safe Coomassie) of End–C–GST for binding partners. *Lane 1*, purified End–C–GST fusion protein (35 kDa); *lane 2*, purified End–C–GST protein after mixing with human brain protein medley, with extra bands for binding proteins shown by *arrows*. (**C**) Example of part of a mass spectrum obtained from tryptic digest of an extra band excised from an SDS-PAGE gel for VD–GST protein binding partners. *x* axis, mass divided by charge; *y* axis, intensity. This peptide mass fingerprint was used with the Mascot search software to identify the proteins in this band, shown in (**D**). Regions in fuzzy print indicate identified fragments. The upper sequence in (**D**) corresponds to β-tubulin (Swiss-Prot P68371) and the lower sequence is α-tubulin (Swiss-Prot P68363) (both these proteins are of similar molecular weight and were present in the same band as a mixture). (**E**) Coimmunoprecipitation of heag2 with interacting proteins. The interaction of the heag2 channel protein with interacting protein is shown using Western blotting with anti-heag2 antibody. *Lane 1*, lysate of HEK293 cells transfected with heag2 (without immunoprecipitation), showing a band at the size corresponding to the expressed heag2 channel protein (115 kDa); *lane 2*, immunoprecipitation with anti-α-tubulin antibody; *lane 3*, immunoprecipitation with anti-heat shock protein antibody; *lane 4*, control, as for lane 2 omitting the anti-α-tubulin antibody

β-tubulins were found to bind, and for the End–C construct myelin basic protein was found to bind. The table also shows the number of peptides identified and the Mascot score. The identified binding proteins and the regions of the heag2 to which they appear to bind are summarized in Fig. 3A.

Immunoprecipitation

The ability of the heag2 channel to bind to human α-tubulin was verified using immunoprecipitation. HEK293 cells were transfected with heag2 and the lysate or coimmunoprecipitated fraction run on SDS-PAGE gels (Fig. 2E). For the cell lysate alone, Western blotting with anti-heag2 antibody showed a clear band at 115 kDa corresponding to heag2 expression (lane 1). Following immunoprecipitation with anti-α-tubulin antibody, Western blotting with anti-heag2 antibody again showed a clear band at 115 kDa corresponding to heag2 (lane 2). This indicates binding between the heag2 protein and endogenous human α-tubulin. The control (lane 4) was obtained as for lane 2 but omitting the anti-α-tubulin antibody and showed the absence of nonspecific binding to the heag2 channel protein. We also showed binding of heat shock protein Hsp70 to heag2 by similar means. The lysate of HEK293 cells cotransfected with heag2 and heat shock protein was immunoprecipitated with anti-Hsp70 antibody. Again, Western blotting with the heag2 antibody showed a clear band at 115 kDa (lane 3).

Taken together, these results further support the proposed interaction of the heag2 channel protein with human α-tubulin and with the heat shock protein family. While not specifically addressing interaction with Hsc71, these experiments do establish binding to the highly homologous (86%) Hsp70 protein. Binding to β-tubulin was not investigated further due to the well-characterized dimeric binding between α- and β-tubulin (Nogales et al. 1998).

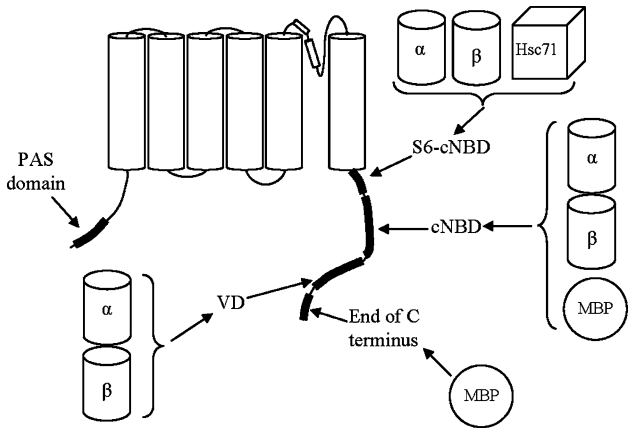

Fig. 3 Schematic representation of the heag2 potassium channel. Regions of the C terminus that were expressed as GST fusion proteins are shown in bold. Binding partners identified by mass spectrometry are shown: α, α-tubulin; β, β-tubulin; MBP, myelin basic protein; Hsc71, heat shock cognate 71-kDa protein

Immunoprecipitation experiments to test for binding of myelin basic protein did not show any evidence of bands for interacting protein (data not shown).

Functional Studies: Electrophysiology

With the interaction between the heag2 potassium channel and human α-tubulin protein confirmed, the functional effect of human α-tubulin on the channel was next studied using two-electrode voltage clamping. Currents from *X. laevis* oocytes injected with RNA for heag2 or α-tubulin or coinjected with both heag2 and α-tubulin RNA were recorded and compared (Fig. 4). *X. laevis* oocytes that were injected with RNA for α-tubulin did not express currents that were significantly different from currents in uninjected cells. The currents recorded from the heag2/α-tubulin coinjected oocytes were outwardly rectifying and noninactivating, characteristic of heag channels (Ju and Wray

Table 1 Identification of heag2 binding proteins

GST fusion protein	Identified protein	SwissProt	Molecular weight (kDa)	Number of peptides matched	Mascot score
S6–cNBD	α-tubulin	P68363	50	12	67
S6–cNBD	β-tubulin	P68371	50	15	61
S6-cNBD	Hsc71	P11142	71	8	54
cNBD	α-tubulin	P68363	50	11	59
cNBD	β-tubulin	P07437	50	11	57
cNBD	MBP	P02686	33	7	71
VD	α-tubulin	P68363	50	15	94
VD	β-tubulin	P68371	50	16	87
End–C	MBP	P02686	33	7	64

The table shows the proteins identified by mass spectrometry as binding to each of the GST fusion constructs. The table also shows the number of peptides matched after tryptic digest and the Mascot score. MBP, myelin basic protein

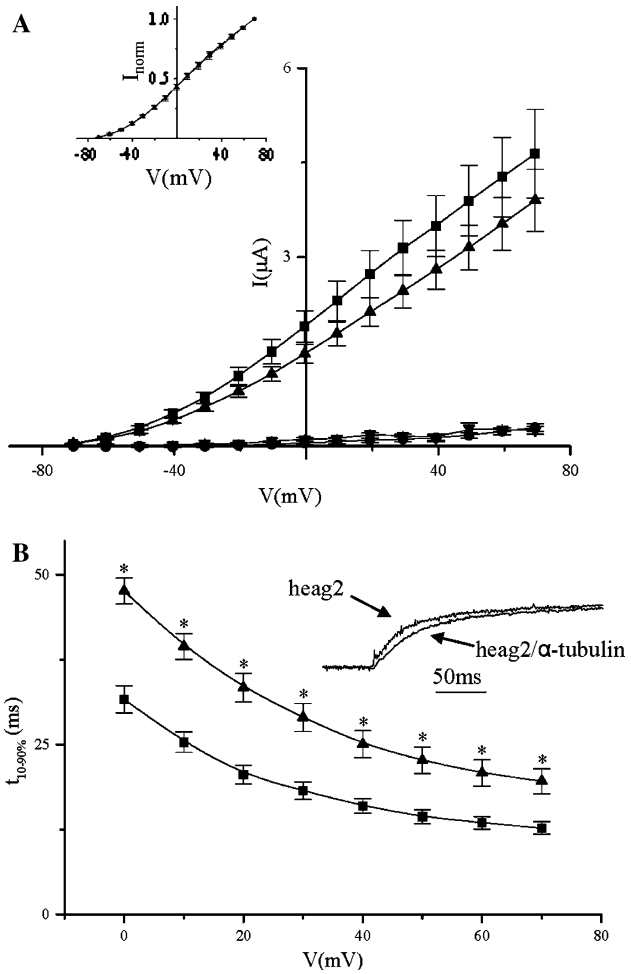

Fig. 4 Effect of α-tubulin on heag2 currents. (**A**) *I–V* curves are shown for cells injected with heag2 RNA (■, $n = 21$), α-tubulin RNA (●, $n = 23$) and heag2/α-tubulin RNA (▲, $n = 30$) and for uninjected oocytes (▼, $n = 5$). Currents for heag2 channels and those recorded from heag2/α-tubulin-coinjected oocytes were not significantly different. Currents for oocytes expressing α-tubulin alone were not significantly different from those for uninjected oocytes. *I–V* curves normalized at + 70 m*V* (*inset, left*) are shown for heag2 channels (■, $n = 21$) and coinjected oocytes (▲, $n = 30$). (**B**) Activation times ($t_{10–90\%}$) for heag2 (■, $n = 21$) and heag2/α-tubulin (▲, $n = 30$) are shown. Values for activation time were significantly different (*$p < 0.05$) at each test potential. Sample currents for steps from −80 to 0 m*V*, normalized to the same maximum, are shown (*inset*) for cells injected with heag2 RNA and coinjected with heag2/α-tubulin RNA

2002). Although current amplitudes appeared to be somewhat smaller for the coinjected oocytes than for those injected with heag2 alone (Fig. 4A), this was not a statistically significant difference. In addition, when the currents for the heag2 channels and the coinjected oocytes were normalized at 70 m*V*, there were no significant differences at any test potential (Fig. 4, inset left), indicating similar voltage dependence. Activation times, $t_{10–90\%}$, for heag2/α-tubulin-coinjected oocytes were significantly increased at each test potential compared with those for heag2 (Fig. 4B), indicating that α-tubulin causes a slowing of channel activation.

To further investigate the effect of α-tubulin on the function of the heag2 channel, the microtubule-disrupting drug colchicine was added to oocytes previously injected with RNA for heag2 or to oocytes coinjected with heag2 and α-tubulin RNA. Oocytes were incubated in Barth's solution containing colchicine (50 μM) for 24 h postinjection, with recordings being made a further 24 h later. Oocytes that had been injected with heag2 RNA and exposed to colchicine expressed currents that were somewhat reduced compared with untreated oocytes expressing heag2 RNA, although this was not statistically significant (Fig. 5A). The current amplitudes recorded from heag2/α-tubulin-coinjected oocytes that were exposed to colchicine were significantly reduced compared to those for heag2/α-tubulin-coinjected oocytes that had not been exposed to colchicine (Fig. 5A). For oocytes expressing heag2 alone, colchicine incubation caused significant increases in activation times (Fig. 6A). There was an apparent slight further slowing in activation time caused by colchicine application to coinjected (heag2/α-tubulin) oocytes, but this was not statistically significant (Fig. 6A).

To investigate the effect of incubation with colchicine at different times, oocytes injected with heag2 RNA or coinjected with heag2/α-tubulin RNA were also exposed to colchicine for 1–5, 24–48 and 43–48 h following RNA injection. The *I–V* relationships for these other colchicine applications are shown in Fig. 5B–D, and the activation times are shown in Fig. 6B–D. It can be seen that each of these three application methods yielded qualitatively similar results to those described above. Thus, while current amplitudes for oocytes expressing heag2 were slightly reduced, though not significantly, by colchicine, those for heag2/α-tubulin coinjected oocytes were consistently reduced, although this was not statistically significant for the 43–48 h exposure protocol. Also, for all times of application, colchicine exposure significantly slowed heag2 channel activation times in oocytes injected with heag2 RNA alone (Fig. 6). The activation times of coinjected (heag2/α-tubulin) oocytes were not significantly affected by colchicine exposure in any of the experiments (Fig. 6). Therefore, colchicine gave a similar pattern of results when applied at different times, although the extent of effects was apparently less for coinjected oocytes exposed to colchicine at 43–48 h.

In order to check for any direct effects of colchicine on the channel itself, we applied colchicine acutely in the bath while recording heag2 currents. After application of colchicine (50 μM) for 5 min, heag2 current amplitudes (3.5 ± 0.8 μA) were not significantly different from initial values (3.5 ± 0.9 μA, $n = 8$). Activation times were not increased after application of colchicine (9.6 ± 0.7 ms) compared with the initial value of activation time

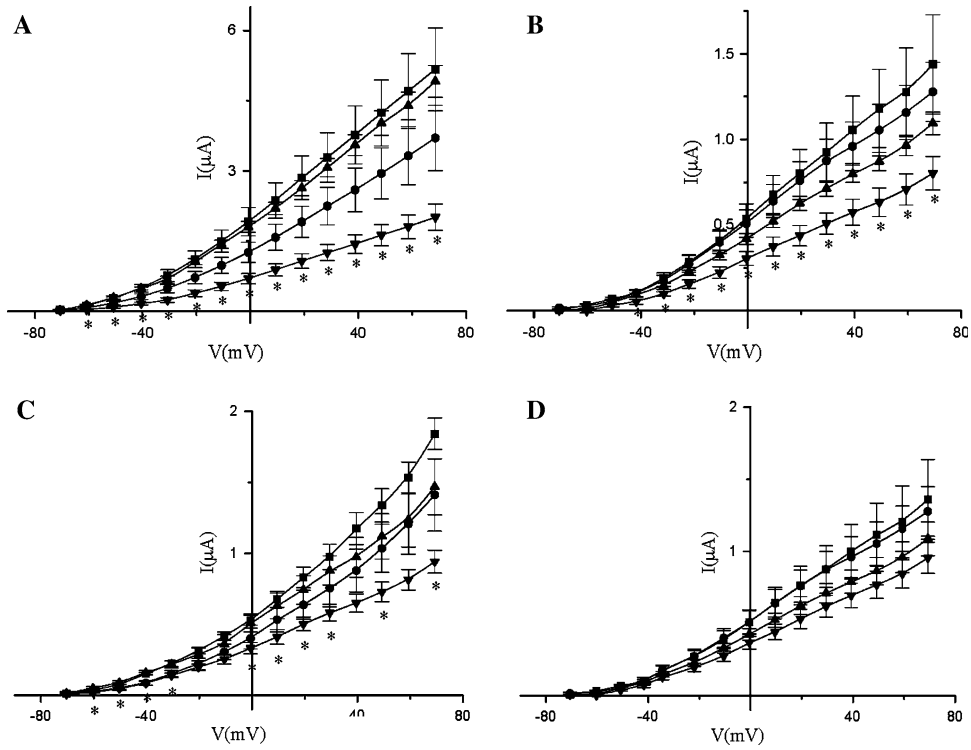

Fig. 5 Effect of colchicine applications on heag2 currents. *I–V* curves are shown for heag2 channels (■), heag2 channels exposed to colchicine (●), coinjected oocytes (heag2/α-tubulin, ▲) and coinjected oocytes (heag2/α-tubulin) exposed to colchicine (▼). Currents from coinjected oocytes treated with colchicine were significantly different from untreated coinjected oocytes at indicated potentials ($^*p < 0.05$). (**A**) Colchicine applied 1–24 h post-RNA injection: ■, $n = 10$; ●, $n = 12$; ▲, $n = 7$; ▼, $n = 10$. (**B**) Colchicine applied 24–48 h post-RNA injection: ■, $n = 12$; ●, $n = 14$; ▲, $n = 11$; ▼, $n = 10$. (**C**) Colchicine applied 1–5 h post-RNA injection: ■, $n = 8$; ●, $n = 7$; ▲, $n = 8$; ▼, $n = 7$. (**D**) Colchicine applied 43–48 h post-RNA injection: ■, $n = 13$; ●, $n = 14$; ▲, $n = 15$; ▼, $n = 11$

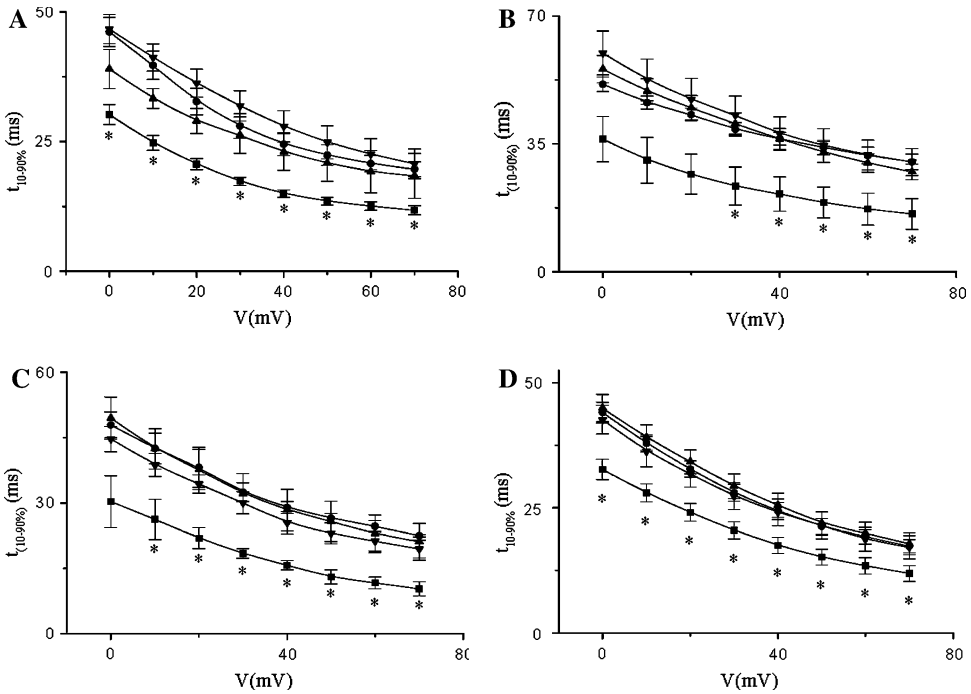

Fig. 6 Effect of colchicine applications on heag2 activation times. Activation times ($t_{10–90\%}$) are shown for heag2 channels (■), heag2 channels exposed to colchicine (●), coinjected oocytes (heag2/α-tubulin, ▲) and coinjected oocytes (heag2/α-tubulin) exposed to colchicine (▼). Values for activation time were significantly different for oocytes injected with heag2 in the presence and absence of colchicine at indicated test potentials, V ($^*p < 0.05$). (**A**) Colchicine applied 1–24 h post-RNA injection: ■, $n = 10$; ●, $n = 12$; ▲, $n = 7$; ▼, $n = 10$. (**B**) Colchicine applied 24–48 h post-RNA injection: ■, $n = 12$; ●, $n = 14$; ▲, $n = 11$; ▼, $n = 10$. (**C**) Colchicine applied 1–5 h post-RNA injection: ■, $n = 8$; ●, $n = 7$; ▲, $n = 8$; ▼, $n = 7$. (**D**) Colchicine applied 43–48 h post-RNA injection: ■, $n = 13$; ●, $n = 14$; ▲, $n = 15$; ▼, $n = 11$

(11.5 ± 0.9 ms), a small but significant ($P < 0.05$) decrease, in contrast to the effect of chronic application of colchicine.

Paclitaxel is a microtubule-stabilizing drug (Moran et al. 2000), so one might predict that contrasting effects to those of colchicine may be observed on heag2 currents. To test this, we incubated oocytes in a bath solution containing paclitaxel (500 nM) for the first 24 h post-RNA injection of heag2 or heag2/α-tubulin. As can be seen from the *I–V* curves in Fig. 7A, paclitaxel did not affect current amplitudes whether for oocytes injected with RNA for heag2 alone or for heag2 and α-tubulin. For activation times, paclitaxel had no effect for oocytes injected with RNA for heag2 alone (Fig. 7B) but gave a significant decrease for heag2 and α-tubulin–coinjected cells. Effects of paclitaxel on both amplitudes and activation times indeed contrast with the effects of colchicine described above.

Finally, we investigated the functional effects of the other potentially interacting proteins identified in the binding studies. When RNA for myelin basic protein was coinjected with heag2, the *I–V* curves and the activation times (Fig. 8A, B) were not significantly different from values for heag2 alone. Similar experiments coexpressing heat shock protein Hsc71 also showed lack of effect on heag2 currents and activation times (Fig. 8C, D). In similar experiments, Hsp70 also did not affect heag2 currents (data not shown). Thus, in contrast to α-tubulin, where clear functional effects were seen (indeed supporting the proposed interaction of tubulin with the channel), no clear functional interaction with the channel was seen for myelin basic protein or heat shock protein.

Discussion

In this study, using a pull-down assay with mass spectrometry, we identified α- and β-tubulin, heat shock protein Hsc71 and myelin basic protein as binding to C-terminal parts of the heag2 potassium channel. Binding to the heag2 channel was also shown by immunoprecipitation for α-tubulin and for a very homologous member of the heat shock 70 protein family, Hsp70, though not for myelin basic protein. Functional effects of α-tubulin coexpression were observed on heag2 currents, with significant slowing of channel activation. Colchicine, when applied chronically (though not acutely), potentiated this effect, while paclitaxel reversed the effect of coexpressed α-tubulin. Neither Hsc71, Hsp70 nor myelin basic protein coexpression with the channel affected channel activation properties.

Three of the heag2–GST fusion proteins, S6–cNBD–GST, cNBD–GST and VD–GST, were found to bind to human tubulin proteins that were identified by mass spectrometry. It is noteworthy that, in each case, both α- and β-tubulin were identified as binding, presumably because of the known tight binding between these two homologous tubulins. Binding of tubulin to GST itself was ruled out by the control experiments, and the immunoprecipitation experiments described above confirmed the binding between heag2 channel protein and the human α-tubulin protein identified from the binding assay.

Coinjection of α-tubulin as well as application of colchicine appeared to show some similar features on the functioning of heag2 channels; in both cases, activation times of the channels were significantly slower. Furthermore, colchicine gave significant reductions in current amplitudes only when heag2 was coexpressed with tubulin. Colchicine acts by binding to free tubulin heterodimers in the cell and also by causing depolymerization of existing microtubules (Pestell 1975; Sackett and Varma 1993). Our data may be understood when it is considered that coexpression of tubulin and application of the drug may have similar effects if it is free tubulin, rather than polymerized tubulin in microtubules, that determines the functional effect on the heag2 channel; both coinjection of α-tubulin

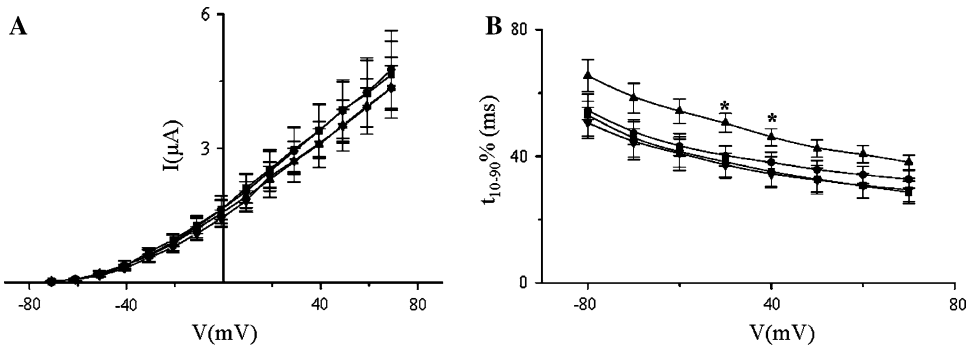

Fig. 7 Effect of paclitaxel on heag2 currents. (**A**) *I–V* curves are shown for cells injected with heag2 RNA (■, $n = 5$), heag2 and exposed to paclitaxel (●, $n = 7$), heag2/α-tubulin RNA (▲, $n = 5$) and heag2/α-tubulin and exposed to paclitaxel (▼, $n = 8$). None of the currents recorded was significantly different at any test potential. (**B**) Activation times ($t_{10–90\%}$) for heag2 (■, $n = 5$), heag2 exposed to paclitaxel (●, $n = 7$), heag2/α-tubulin (▲, $n = 5$) and heag2/α-tubulin exposed to paclitaxel (▼, $n = 8$). Values for activation time of heag2/α-tubulin currents and heag2/α-tubulin exposed to paclitaxel currents were significantly different ($*p < 0.05$) at test potentials, V

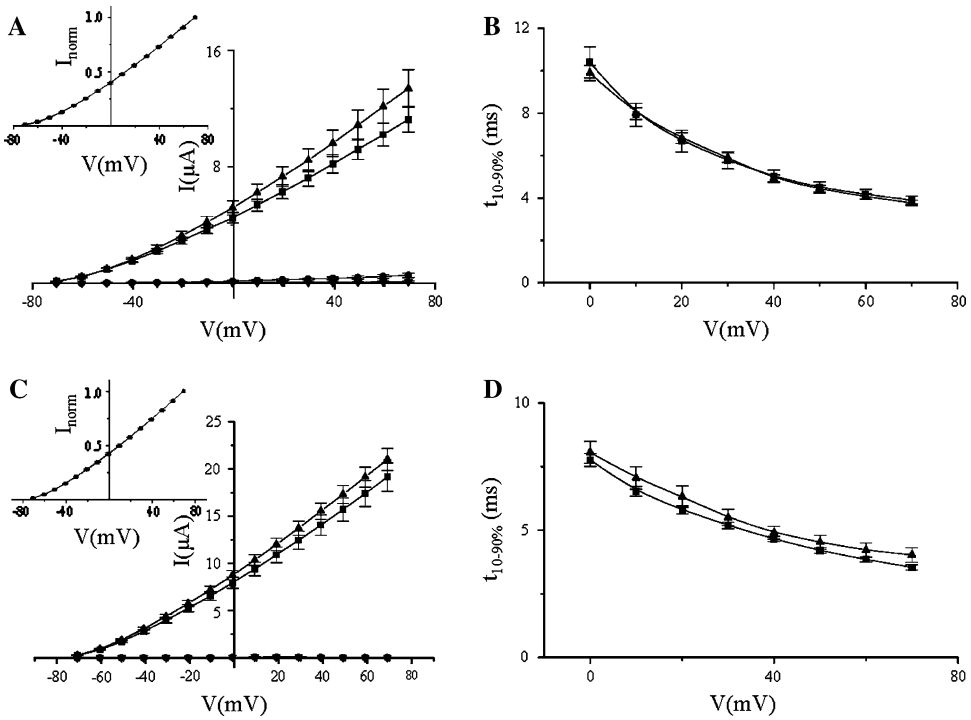

Fig. 8 Effect of myelin basic protein and heat shock protein on heag2 currents. (**A**) *I–V* curves are shown for cells injected with heag2 RNA (■, $n = 22$), myelin basic protein RNA (●, $n = 20$) and heag2/myelin basic protein RNA (▲, $n = 32$) and for uninjected oocytes (▼, $n = 9$). Currents for heag2 channels and those recorded from heag2/myelin basic protein–coinjected oocytes were not significantly different. Currents for oocytes expressing myelin basic protein alone were not significantly different from those for uninjected oocytes. *I–V* curves normalized at + 70 m*V* (*inset, left*) are shown for heag2 channels (■, $n = 22$) and coinjected oocytes (▲, $n = 32$). (**B**) Activation times ($t_{10–90\%}$) for heag2 (■, $n = 22$) and heag2/myelin basic protein (▲, $n = 32$) are shown. Values for activation time were not significantly different at any test potential. (**C**) *I–V* curves are shown for cells injected with heag2 RNA (■, $n = 26$), Hsc71 RNA (●, $n = 14$) and heag2/Hsc71 RNA (▲, $n = 31$) and for uninjected oocytes (▼, $n = 8$). Currents for heag2 channels and those recorded from heag2/Hsc71–coinjected oocytes were not significantly different. Currents for oocytes expressing Hsc71 alone were not significantly different from those for uninjected oocytes. *I–V* curves normalized at + 70 m*V* (*inset, left*) are shown for heag2 channels (■, $n = 26$) and coinjected oocytes (▲, $n = 31$). (**D**) Activation times ($t_{10–90\%}$) for heag2 (■, $n = 26$) and heag2/Hsc71 (▲, $n = 31$) are shown. Values for activation time were not significantly different at any test potential

and application of colchicine increase free tubulin concentration. This interpretation of free tubulin causing the functional effects is further supported by our experiments with paclitaxel, which stabilizes microtubules rather than destabilizing them like colchicine (Huzil et al. 2006). Indeed, the effect of paclitaxel was to reverse the slowing effect of tubulin coexpression on activation kinetics. The suggestion that free tubulin can interact with an ion channel has also been proposed by van Rossum, Kuhse and Betz (1999) for the NMDA receptor channel.

Another possibility is that the trafficking of heag2 channels to the membrane is inhibited through disruption of the microtubules of the cytoskeleton by colchicine. Although we did not directly measure surface expression, application of colchicine for different durations showed similar results, pointing to lack of effect of colchicine on trafficking. More importantly, a further indication that the action of injected α-tubulin RNA and/or colchicine is not primarily the result of defective trafficking is that the channel activation times are altered by these agents. The lack of major effect of tubulin and colchicine on trafficking is consistent with data for other ion channels, such as sodium and calcium channels (Galli and DeFelice 1994; Moran et al. 2000). A further mechanism for the effect of colchicine could be via a direct action of the drug on the heag2 channel. However, our results for direct application of colchicine in the bath showed no effect on current amplitudes and no slowing of activation as observed in any of the chronic applications, suggesting lack of direct action of colchicine. Also, studies on other channels have not reported direct actions of colchicine (or the microtubule stabilizer taxol) (Galli and DeFelice 1994; Camacho et al. 2000; Moran et al. 2000). Yet another mechanism for the action of colchicine may be through microtubule-induced disruption of the microvillae (Massover 1973) present in oocyte membranes, leading to a decrease in oocyte cell membrane area and whole-cell currents. However, reversal of this effect by tubulin RNA injection was not observed, and in any case the changes in activation times by colchicine and/or tubulin cannot be explained by such a mechanism.

Although it seems likely that free tubulin is the factor leading to functional effects on the heag2 channel, it is not clear whether the action of tubulin on the channel is direct or is mediated through an intermediary protein. Intermediary proteins have been identified for other ion channels that interact with tubulin, including GABA receptors (Wang et al. 1999; Chen et al. 2000) and glycine receptors (Kirsch et al. 1991). However, the heag2 channel lacks a recognized tubulin-binding domain, such as that found on other proteins like $GABA_A$ receptor–associated protein (Wang et al. 1999). For the heag2 channel, there may be multiple intermediate proteins since we observed clear binding to several distinct regions in the C terminus. A further possibility could be the induction by tubulin overexpression of another protein that interacts with heag2. On the other hand, direct binding of tubulin has been proposed for the NMDA channel despite it lacking a known consensus tubulin binding sequence (van Rossum et al. 1999). Perhaps arguing against direct binding could be the fact that tubulin appeared to bind to several fragments, even though there are no apparently similar sequences in the fragments.

It will therefore be interesting to investigate whether direct binding of tubulin to the channel occurs, e.g., by biochemical binding studies with purified, tagged proteins. Even though we were careful to choose some of the binding fragments homologous to known domains whose structure is known (see "Methods"), a possible limitation of our results could be lack of native configuration of some of the domains used as fragments, with perhaps spurious results. Further experimental investigation would need to be carried out to address these points.

While the precise mechanism of interaction of the heag2 channel and α-tubulin is not clear, it is apparent that these proteins are intimately linked to one another. Both microtubules (Hyams and Lloyd 1993) and potassium channels (Pardo 2004; Lang et al. 2005) are involved in cell proliferation. Indeed, normal and pathological cell proliferation have been linked to potassium channels such as eag1 and herg (Bruggemann et al. 1997; Pardo et al. 1998, 1999; Bianchi et al. 1998; Camacho et al. 2000; Wang 2004; Patel and Lazdunski 2004), and our data suggest that the heag2 channel may also have a physiological role in cell proliferation via interaction with microtubules, perhaps via the intermediary of free tubulin. With many forms of cancer being found to have links to herg and heag1 channels (Camacho 2006), the suggestion of a further channel, heag2, being involved with cellular proliferation through cytoskeletal interaction may be worthy of further investigation.

We have also identified heat shock 70 proteins (Hsc71 and Hsp70) in our binding studies, although neither protein affected heag2 channel currents in coexpression studies. Heat shock proteins function as molecular chaperones involved in protein folding and trafficking (Schlossman et al. 1984; Chappell et al. 1986; Chirico, Waters and Blobel 1988). Thus, it seems highly likely that heat shock proteins indeed play a role in heag2 cellular trafficking. It may be that levels of constitutively expressed Hsc71 are already high in the cell, and further coexpression would therefore make little difference to expression level and channel currents, as we observed. It is of interest that Hsc71 appears to be involved in trafficking of another member of the ether-a-go-go family (herg) (Ficker et al. 2003), lending further support to our suggestion of a role for heat shock proteins in heag2 trafficking.

Our mass spectrometric analysis of binding partners also identified myelin basic protein. This protein is widely distributed in the brain and appears to be involved in many processes besides simply a role in myelination (Givorgi et al. 2000). Myelin basic protein and microtubules are closely associated in oligodendrocytes (Wilson and Brophy 1989), and the protein forms complexes with tubulin (Modesti and Barra 1986). It is therefore possible that the interaction between heag2 and tubulin previously discussed is linked to the association of myelin basic protein with the channel. However, we were unable to confirm binding of myelin basic protein by immunoprecipitation, and coexpression experiments indicated no functional effect on heag2 currents. Thus, a possible interpretation of our results is that we picked up nonspecific binding of the abundantly expressed myelin basic protein in our mass spectrometric analysis. In contrast though, we did not detect other abundant proteins such as actins and cytokeratins, which would perhaps have been pulled down if our assays had been prone to detecting nonspecific binding.

In summary, we have identified tubulins and heat shock proteins as binding to parts of the heag2 intracellular C terminus. We were also able to show functional effects of tubulins on the channel. Our work suggests a role for the heag2 channel in cytoskeletal interactions.

Acknowledgements This work was funded by the Biotechnology and Biological Sciences Research Council. We thank E. Morrison for advice and M. Peckham and S. Dunn for help with the immunoprecipitation experiments. The mass spectrometry was carried out by J. Keen in the Faculty Proteomics Facility, funded by a Joint Research Equipment Initiative to J. B. C. Findlay.

References

Bauer CK, Schwarz JR (2001) Physiology of EAG K^+ channels. J Membr Biol 182:1–15

Bianchi L, Wible B, Arcangeli A, Taglialatela M, Morra F, Castaldo P, Crociani O, Rosati B, Faravelli L, Olivotto M, Wanke E

(1998) HERG encodes a K^+ current highly conserved in tumors of different histogenesis: a selective advantage for cancer cells? Cancer Res 58:815–822

Bracey K, Wray D (2006) Inherited disorders of ion channels. In: Voltage-gated ion channels as drug targets, Wiley-VCH, New York

Bruggemann A, Stuhmer W, Pardo LA (1997) Mitosis-promoting factor-mediated suppression of a cloned delayed rectifier potassium channel expressed in *Xenopus* oocytes. Proc Natl Acad Sci USA 94:537–542

Camacho J (2006) Ether a go-go potassium channels and cancer. Cancer Lett 233:1–9

Camacho J, Sánchez A, Stühmer W, Pardo LA (2000) Cytoskeletal interactions determine the electrophysiological properties of human EAG potassium channels. Pfluegers Arch 441:167–174

Chappell TG, Welch WJ, Schlossman DM, Palter KB, Shlesinger MJ, Rothman JE (1986) Uncoating ATPase is a member of the 70 kilodalton family of stress proteins. Cell 45:3–13

Chen L, Wang H, Vicini S, Olsen RW (2000) The gamma-aminobutyric acid type A (GABAA) receptor-associated protein (GABARAP) promotes GABAA receptor clustering and modulates the channel kinetics. Proc Natl Acad Sci USA 97:11557–11562

Chirico WJ, Waters MG, Blobel G (1988) 70K heat shock related proteins stimulate protein translocation into microsomes. Nature 332:805–810

Farias LMB, Ocana DB, Diaz L, Larrea F, Avila-Chavez E, Cadena A, Hinojosa LM, Lara G, Villanueva LA, Vargas C, Hernandez-Gallegos E, Camacho-Arroyo I, Duenas-Gonzalez A, Perez-Cardenas E, Pardo LA, Morales A, Taja-Chayeb L, Escamilla J, Sanchez-Pena C, Camacho J (2004) Ether a go-go potassium channels as human cervical cancer markers. Cancer Res 64:6996–7001

Ficker E, Dennis AT, Wang L, Brown AM (2003) Role of the cytosolic chaperones Hsp70 and Hsp90 in maturation of the cardiac potassium channel HERG. Circ Res 92:e87–e100

Galli A, DeFelice LJ (1994) Inactivation of L-type Ca channels in embryonic chick ventricle cells: dependence on the cytoskeletal agents colchicine and taxol. Biophys J 67:2296–2304

Givogri MI, Bongarzone ER, Campagnoni AT (2000) New insights on the biology of myelin basic protein gene: the neural–immune connection. J Neurosci Res 59:153–159

Huzil JT, Luduena RF, Tuszynski J (2006) Comparative modeling of human beta tubulin isotypes and implications for drug binding. Nanotechnology 17:S90–S100

Hyams JS, Lloyd CW (1993). Microtubules. Wiley-Liss, New York

Ju M, Wray D (2002) Molecular identification and characterisation of the human eag2 potassium channel. FEBS Lett 524:204–210

Ju M, Wray D (2006) Molecular regions responsible for differences in activation between heag channels. Biochem Biophys Res Commun 342:1088–1097

Ju M, Stevens L, Leadbitter E, Wray D (2003) The roles of N- and C-terminal determinants in the activation of the Kv2.1 potassium channel. J Biol Chem 278:12769–12778

Kirsch J, Langosch D, Prior P, Littauer UZ, Schmitt B, Betz H (1991) The 93-kDa glycine receptor-associated protein binds to tubulin. J Biol Chem 266:22242–22245

Lang F, Föller M, Lang KS, Lang PA, Ritter M, Gulbins E, Vereninov A, Huber SM (2005) Ion channels in cell proliferation and apoptotic cell death. J Membr Biol 205:147–157

Massover WH (1973) Complex surface invaginations in frog oocytes. J Cell Biol 58:485–491

Mello de Queiroz F, Suarez-Kurtz G, Stuhmer W, Pardo LA (2006) Ether a go-go potassium channel expression in soft tissue sarcoma patients. Mol Cancer 5:42–54

Modesti NM, Barra HS (1986) The interaction of myelin basic protein with tubulin and the inhibition of tubulin carboxypeptidase activity. Biochem Biophys Res Commun 136:482–489

Moran O, Tammaro P, Nizzari M, Conti F (2000) Functional properties of sodium channels do not depend on the cytoskeleton integrity. Biochem Biophys Res Commun 276:204–209

Nogales E, Wolf SG, Downing KH (1998) Structure of the alpha beta tubulin dimer by electron crystallography. Nature 391:199–203

Pardo LA (2004) Voltage-gated potassium channels in cell proliferation. Physiology 19:285–292

Pardo LA, Brüggemann A, Camacho J, Stühmer W (1998) Cell cycle-related changes in the conducting properties of r-eag K^+ channels. J Cell Biol 143:767–775

Pardo LA, del Camino D, Sánchez A, Alves F, Brüggemann A, Beckh S, Stühmer W (1999) Oncogenic potential of EAG K^+ channels. EMBO J 18:5540–5547

Patel AJ, Lazdunski M (2004) The 2P-domain K^+ channels: role in apoptosis and tumorigenesis. Pfluegers Arch 448:261–273

Perkins DN, Pappin DJ, Creasy DM, Cottrell JS (1999) Probability-based protein identification by searching sequence databases using mass spectrometry data. Electrophoresis 20:3551–3567

Pestell RQW (1975) Microtubule protein synthesis during oogenesis and early embryogenesis in *Xenopus laevis*. Biochem J 145:527–534

Sackett DL, Varma JK (1993) Molecular mechanism of colchicine action: induced local unfolding of beta-tubulin. Biochemistry 32:13560–13565

Schlossman DM, Schmid SL, Braell WA, Rothman JE (1984) An enzyme that removes clathrin coats: purification of an uncoating ATPase. J Cell Biol 99:723–733

Schönherr R, Gessner G, Löber K, Heinemann SH (2002) Functional distinction of human EAG1 and EAG2 potassium channels. FEBS Lett 514:204–208

Toral C, Mendoza-Garrido ME, Azorin E, Hernandez-Gallegos E, Gomora JC, Delgadillo DM, Solano-Agama C, Camacho J (2007) Effect of extracellular matrix on adhesion, viability, actin cytoskeleton and K^+ currents of cells expressing human ether a go-go channels. Life Sci 81:255–265

van Rossum D, Kuhse J, Betz H (1999) Dynamic interaction between soluble tubulin and C-terminal domains of N-methyl-D-aspartate receptor subunits. J Neurochem 72:962–973

Venter H, Ashcroft AE, Keen JN, Henderson PJ, Herbert RB (2002) Molecular dissection of membrane-transport proteins: mass spectrometry and sequence determination of the galactose-H^+ symport protein, GalP, of *Escherichia coli* and quantitative assay of the incorporation of [ring-2–13C]histidine and (15)NH(3). Biochem J 363(Pt 2):243–252

Wang Z (2004) Roles of K^+ channels in regulating tumour cell proliferation and apoptosis. Pfluegers Arch 448:274–286

Wang H, Bedford FK, Brandon NJ, Moss SJ, Olsen RW (1999) GABA(A)-receptor-associated protein links GABA(A) receptors and the cytoskeleton. Nature 397:69–72

Wilson R, Brophy PJ (1989) Role for the oligodendrocyte cytoskeleton in myelination. J Neurosci Res 22:439–448

Yellen G (2002) The voltage-gated potassium channels and their relatives. Nature 419:35–42

Zagotta WN, Olivier NB, Black KD, Young EC, Olson R, Gouaux E (2003) Structural basis for modulation and agonist specificity of HCN pacemaker channels. Nature 425:200–205